

Crystal structure and Hirshfeld surface analysis of *N*-{*N*-[amino(dimethylamino)methyl]carbamimidoyl}-3-bromobenzenesulfonamide

Kexin Su,^a Jiangshui Luo^b and Luc Van Meervelt^{a*}

^aDepartment of Chemistry, KU Leuven, Biomolecular Architecture, Celestijnenlaan 200F, Leuven (Heverlee), B-3001, Belgium, and ^bCollege of Materials Science and Engineering, Sichuan University, Chengdu, 610065, People's Republic of China. *Correspondence e-mail: luc.vanmeervelt@kuleuven.be

Received 1 March 2023

Accepted 7 March 2023

Edited by S. Parkin, University of Kentucky, USA

Keywords: crystal structure; metformin; hydrogen-bond interactions; π - π interactions; Hirshfeld surface analysis.

CCDC reference: 2246792

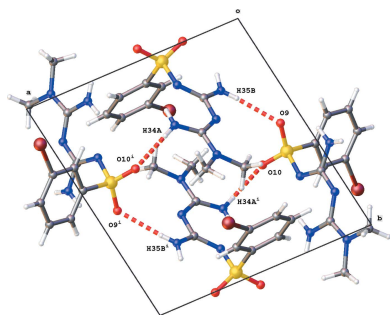
Supporting information: this article has supporting information at journals.iucr.org/e

The title compound, $C_{10}H_{14}BrN_5O_2S$, is the bromobenzenesulfonamide derivative of the type 2 diabetes drug metformin. The asymmetric unit contains two molecules with almost identical conformations but a different orientation of the bromophenyl moiety. Both molecules exhibit intramolecular $N-H \cdots N$ and $N-H \cdots O$ hydrogen bonds. The molecular packing features chain formation in the *a*-axis direction by alternating $N-H \cdots N$ and $N-H \cdots O$ interactions. In addition, ring motifs consisting of four molecules and π - π interactions between the phenyl rings contribute to the three-dimensional architecture. A Hirshfeld surface analysis shows that the largest contributions to surface contacts arise from contacts in which H atoms are involved.

1. Chemical context

Metformin is a widely known effective drug for type 2 diabetes, which does not cause weight gain and rarely causes hypoglycemia. Metformin works by decreasing gluconeogenesis in the liver, increasing insulin sensitivity and preventing insulin resistance (Giannarelli *et al.*, 2003). In addition to antidiabetics, metformin shows confirmed benefits against aging (Barzilai *et al.*, 2016) and various diseases such as polycystic ovary syndrome (Lord *et al.*, 2003), cancers (Libby *et al.*, 2009), obesity (Jing *et al.*, 2018), liver disease (Lin *et al.*, 2000) and cardiovascular disease (Rena & Lang, 2018). In recent decades, there has been great interest in metformin because of its multiple medical applications and low toxicity. However, metformin also has some disadvantages, such as low bioavailability, incomplete absorption, and gastrointestinal side effects. Gliclazide is an oral sulfonylurea antidiabetic agent that works by stimulating insulin synthesis (Sarkar *et al.*, 2011). We think that the combination of the two with different mechanisms of action can synergize and result in a potent hypoglycemic effect. In addition, the combination can improve their physico-chemical properties and alleviate the side effects caused by high doses of a single drug.

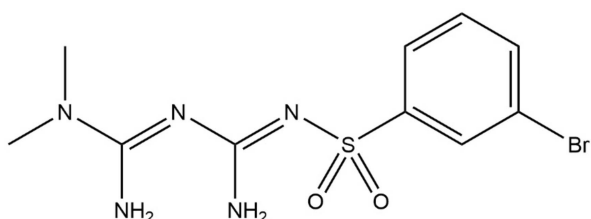
Introducing sulfonyl into small medical molecules is an important strategy in modifying the molecular structure of drugs. Sulfonyl can provide two hydrogen-bond acceptors, and the introduction of the sulfonyl group can improve the bioactivity of the compound by increasing the hydrogen-bond interactions between drug and target. In addition, the sulfonyl group has a relatively stable structure, and the introduction of sulfonyl can block easily metabolizable sites and prolong its time of action, improving its bioavailability, and thereby



OPEN ACCESS

Published under a CC BY 4.0 licence

improving the pharmacokinetic properties of small molecules. In summary, it makes sense to synthesize ion pairs of gliclazide and sulfonyl-modified metformin and investigate its pharmaceutical properties. Herein we report the crystal structure and Hirshfeld surface analysis of the title compound, $C_{10}H_{14}BrN_5O_2S$, obtained during our efforts to crystallize the ion pair with gliclazide.



2. Structural commentary

The title compound crystallizes in the triclinic space group $P\bar{1}$ with two molecules (*A* containing S8 and *B* containing S27) in the asymmetric unit (Fig. 1). Although both molecules have an

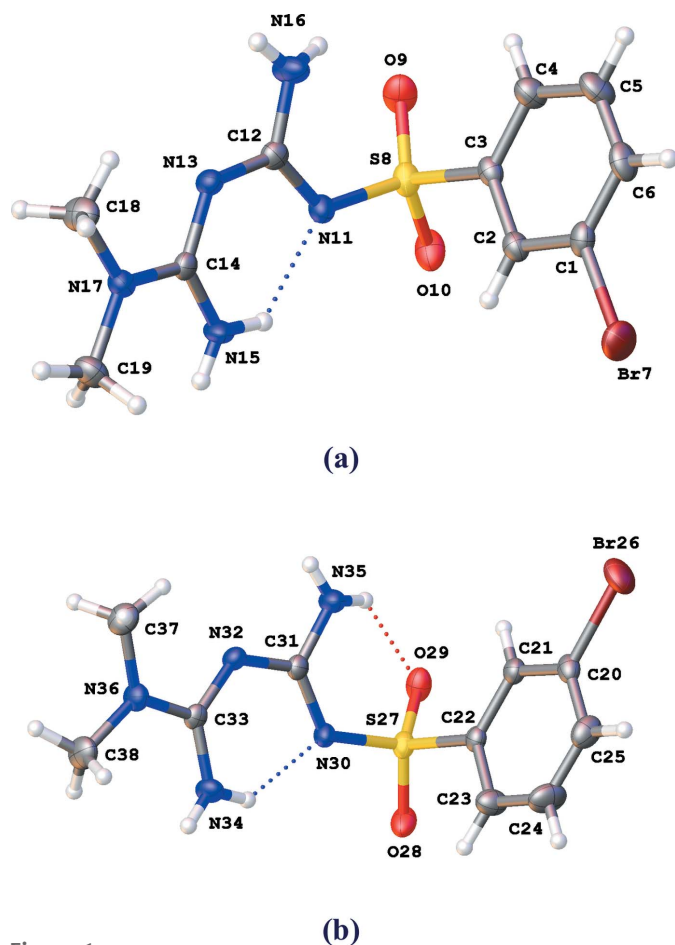


Figure 1
The molecular structure of the two independent molecules (*A* and *B*) of the title compound, showing the atom labelling scheme. Displacement ellipsoids are drawn at the 30% probability level. Only the major component is shown. Intramolecular interactions are shown as dotted lines.

Table 1
Hydrogen-bond geometry (\AA , $^\circ$).

$D-H\cdots A$	$D-H$	$H\cdots A$	$D\cdots A$	$D-H\cdots A$
$N15-H15B\cdots N11$	0.86 (6)	2.02 (6)	2.655 (6)	130 (5)
$N16-H16B\cdots O9$	0.83 (6)	2.19 (5)	2.830 (6)	134 (5)
$N34-H34B\cdots N30$	0.86 (6)	2.02 (6)	2.696 (5)	135 (5)
$N35-H35A\cdots O29$	0.83 (5)	2.18 (5)	2.823 (6)	136 (4)
$N35-H35B\cdots O9$	0.78 (5)	2.27 (5)	3.049 (6)	175 (5)
$N16-H16A\cdots N32^i$	0.81 (5)	2.54 (5)	3.225 (6)	144 (4)
$N34-H34A\cdots O10^{ii}$	0.85 (5)	2.23 (5)	3.063 (5)	165 (4)

Symmetry codes: (i) $-x, -y + 1, -z + 1$; (ii) $-x + 1, -y + 1, -z + 1$.

almost identical conformation, the bromophenyl part shows two orientations related by a rotation of 180° (Fig. 2). The hydrogen atoms involved in the intramolecular hydrogen bonds $N11\cdots N15$ (molecule *A*) and $N30\cdots N34$ (molecule *B*) are shared by the two nitrogen atoms with an occupancy of 0.85 (4) at atoms $N15$ and $N34$, and 0.15 (4) at atoms $N11$ and $N30$. The dihedral angles between the phenyl ring ($C1-C6$ in *A*, $C20-C25$ in *B*) and the best plane through the N-containing moiety ($N11-C19$ in *A* and $N30-C38$ in *B*) are 87.12 (12) and 96.05 (12) $^\circ$ in *A* and *B*, respectively. Next to the intramolecular hydrogen bonds $N15-H15B\cdots N11$ and $N34-H34B\cdots N30$, a short interaction is present between atoms $H16B$ and $O9$ in *A*, and $H35B$ and $O9$ in *B* (Table 1).

3. Supramolecular features

The crystal packing of the title compound is characterized by $N-H\cdots N$, $N-H\cdots O$ and $\pi-\pi$ interactions. The two molecules *A* and *B* in the asymmetric unit are linked by an $N35-H35B\cdots O9$ interaction (Table 1). Molecule *A* interacts with a second molecule *B* by an $N16-H16A\cdots N32(-x, -y + 1, -z + 1)$ interaction, while molecule *B* forms an $N34-H34A\cdots O10(-x + 1, -y + 1, -z + 1)$ hydrogen-bond interaction (Table 1). These dimers [graph-set notation $D_1^1(2)$; Etter & MacDonald, 1990] are the building blocks for a three-dimensional network consisting of chains [graph-set notation $C_2^2(10)$] and rings [graph-set notation $R_4^4(20)$]. A chain running in the *a*-axis direction is formed by subsequent $N16\cdots N32$ and $N34\cdots O10$ interactions (Fig. 3). One ring motif consists of

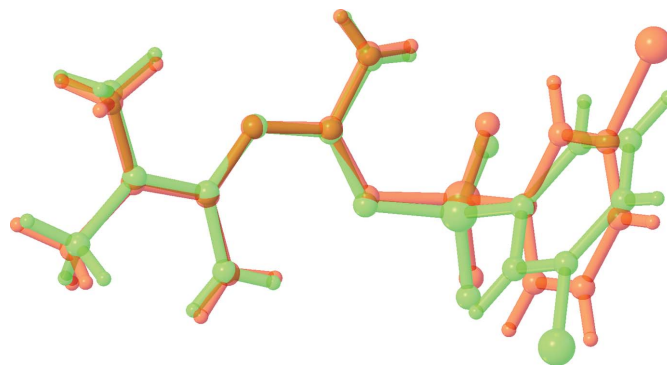


Figure 2
A view of the molecular fit of the *A* (green) and *B* (orange) molecules of the title compound (major component) calculated using the Overlay routine in OLEX2 (Dolomanov *et al.*, 2009).

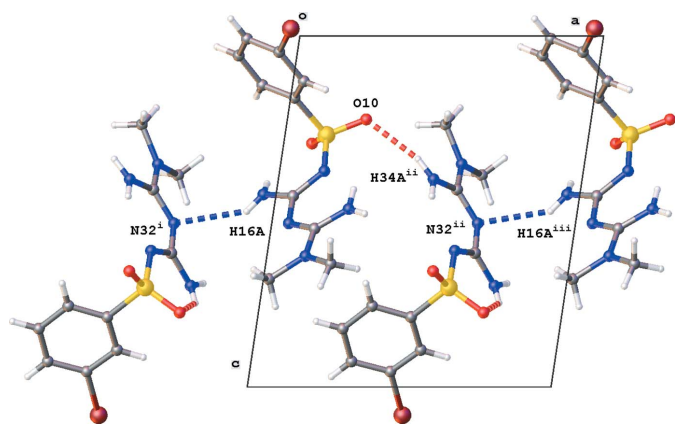


Figure 3
 Partial crystal packing of the title compound, showing the chain formation in the *a*-direction. N–H···N and N–H···O hydrogen bonding are shown as blue and red dashed lines, respectively. Symmetry codes: (i) $-x, -y + 1, -z + 1$, (ii) $-x + 1, -y + 1, -z + 1$, (iii) $x + 1, y, z$.

N16···N32 and N35···O9 interactions (Fig. 4), while N34···O10 and N35···O9 interactions result in the second ring motif (Fig. 5).

Further dimer formation is obtained through π – π stacking between the phenyl rings (Fig. 6). For molecule *A*, the Cg1···Cg1($-x, -y + 1, -z$) distance is 3.686 (3) Å and the slippage is 0.650 Å, while for molecule *B* the Cg2···Cg2($-x + 1, -y, -z$) distance is 4.1086 (3) Å and the slippage is 1.936 Å (Cg1 and Cg2 are the centroids of rings C1–C6 and C20–C25, respectively).

A Hirshfeld surface analysis was performed, and two-dimensional fingerprint plots were created with *Crystal*

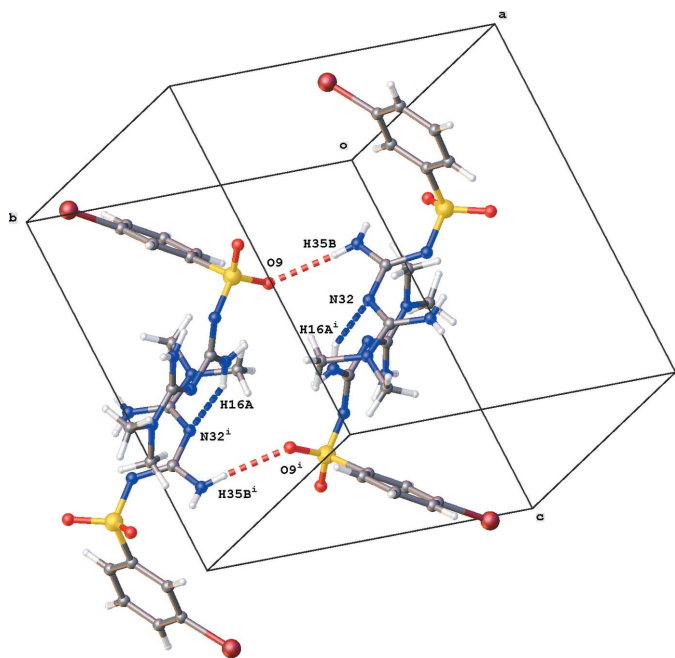


Figure 4
 Partial crystal packing of the title compound, showing $R_4^2(20)$ ring formation through N–H···N and N–H···O hydrogen bonding shown as blue and red dashed lines, respectively. Symmetry code: (i) $-x, -y + 1, -z + 1$.

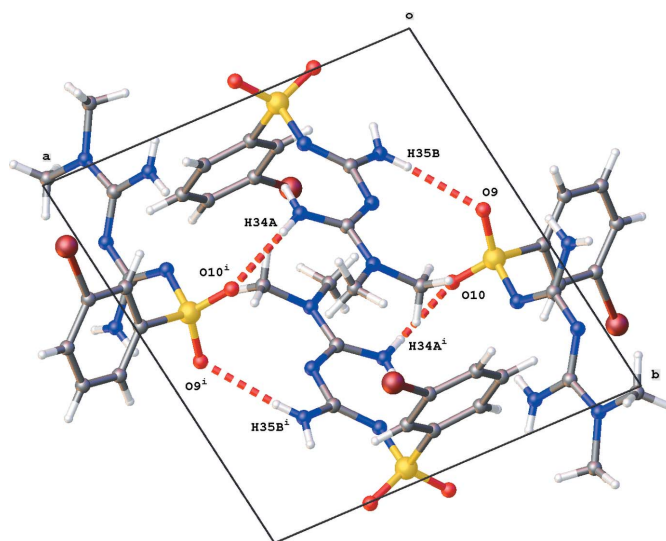


Figure 5
 Partial crystal packing of the title compound, showing $R_4^2(20)$ ring formation through N–H···O hydrogen bonding shown as red dashed lines. Symmetry code: (i) $-x + 1, -y + 1, -z + 1$.

Explorer21.3 (Spackman *et al.*, 2021). The Hirshfeld surfaces of molecules *A* and *B* mapped over d_{norm} are given in Figs. 7 and 8, respectively. The bright-red spots in Fig. 7 near atoms O9 and O10 are indicative of the N34–H34A···O10 and

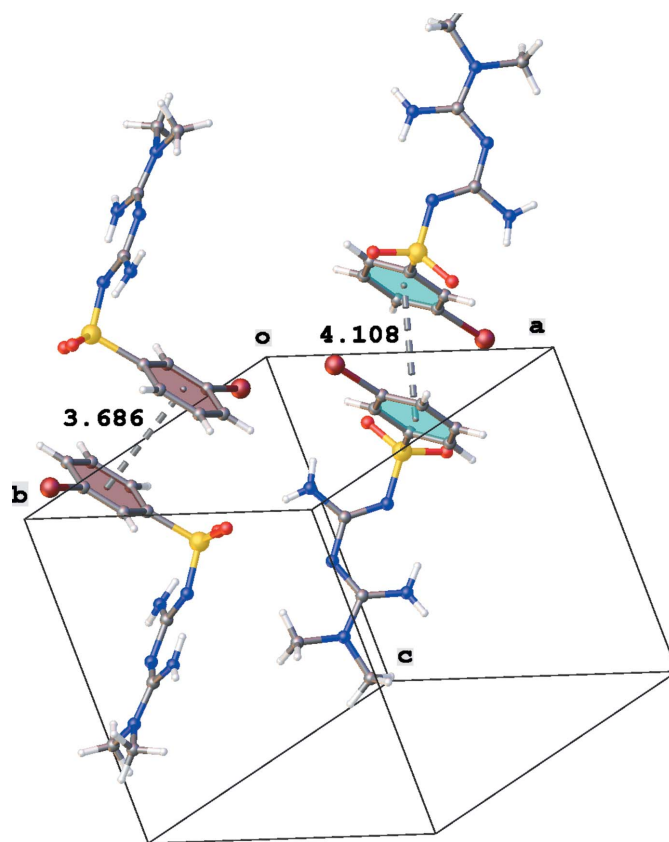


Figure 6
 Partial crystal packing of the title compound, showing the π – π stacking between the phenyl rings. Centroid to centroid distances are given in Å.

N35–H35B···O9 hydrogen bonds, while the additional faint-red spots illustrate weaker C14···H23 (2.66 Å), H16A···N32 [2.54 (5) Å] and Br···Br [3.4165 (10) Å] interactions present in the crystal packing. The bright-red spots in Fig. 8 near atoms N32, H34A and H35B refer to the N16–H16A···N32, N34–H34A···O10 and N35–H35B···O9 hydrogen bonds, while the additional faint-red spots illustrate weaker H15A···N30 [2.70 (5) Å] and C14···H23 (2.66 Å) interactions present in the crystal packing. The relative distributions from the different interatomic contacts to the Hirshfeld surfaces are presented in Table 2. The most significant contributions to the Hirshfeld surface are H···H (35.0%, 34.0%), O···H/H···O (19.2%, 17.7%), H···Br/Br···H (14.1%, 14.6%), H···C/C···H (13.1%, 15.0%), and H···N/N···H (11.5%, 10.5%) contacts (values for molecule *A* and *B*, respectively).

4. Database survey

A search of the Cambridge Structural Database (CSD, Version 5.43, update of November 2022; Groom *et al.*, 2016)

Table 2

Percentage contributions of interatomic contacts to the Hirshfeld surfaces for molecules *A* and *B*.

Contact	Molecule <i>A</i>	Molecule <i>B</i>
C···C	3.2	2.4
C···H/H···C	13.1	15.0
H···H	35.0	34.0
Br···C/C···Br	0.2	2.1
Br···H/H···Br	14.1	14.6
Br···Br	1.7	0.0
S···C/C···S	0.0	0.0
S···H/H···S	0.1	0.1
S···Br/Br···S	0.0	0.0
S···S	0.0	0.0
O···C/C···O	0.4	0.0
O···H/H···O	19.2	17.7
O···Br/Br···O	0.8	2.9
O···S/S···O	0.0	0.0
O···O	0.1	0.1
N···C/C···N	0.3	0.2
N···H/H···N	11.5	10.5
N···Br/Br···N	0.0	0.0
N···S/S···N	0.0	0.0
N···O/O···N	0.0	0.0
N···N	0.2	0.4

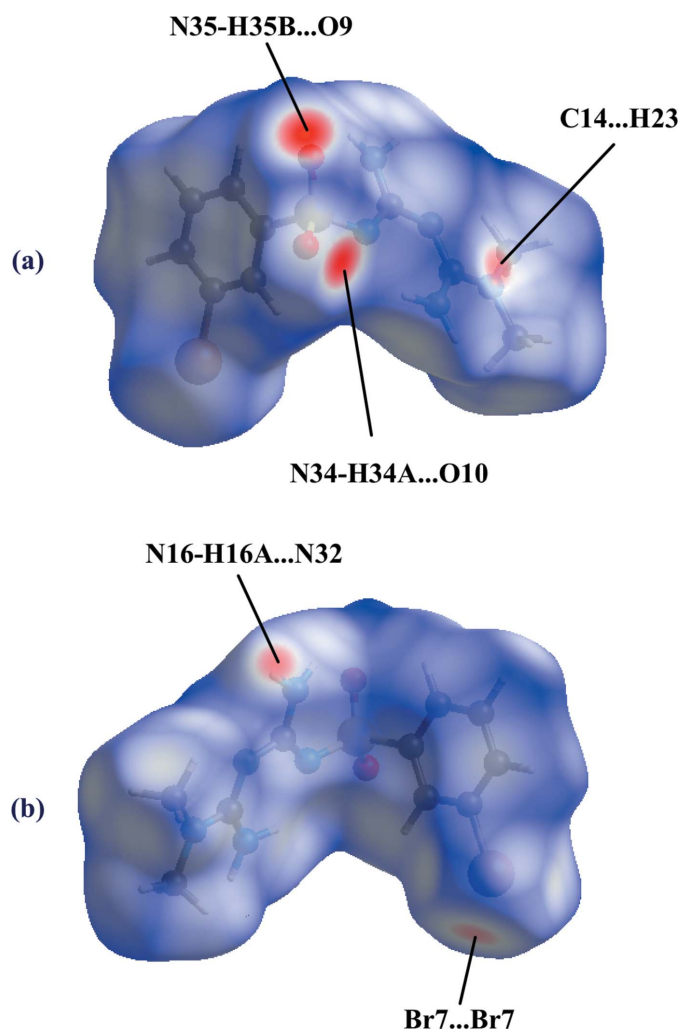


Figure 7
The Hirshfeld surface for molecule *A* mapped over d_{norm} : (a) front view, (b) back view.

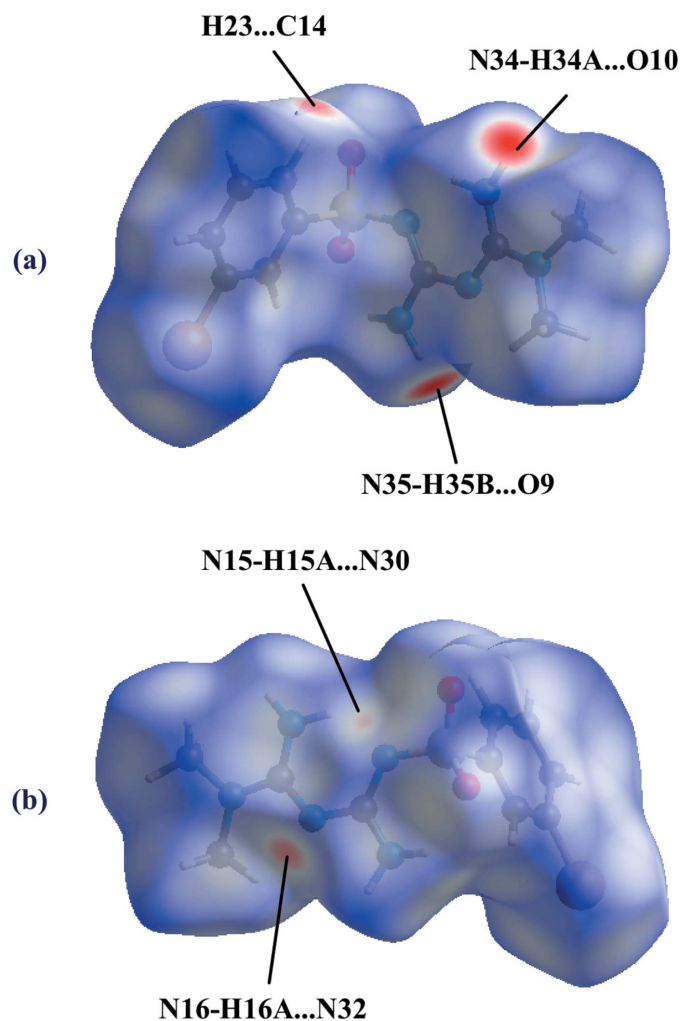


Figure 8
The Hirshfeld surface for molecule *B* mapped over d_{norm} : (a) front view, (b) back view.

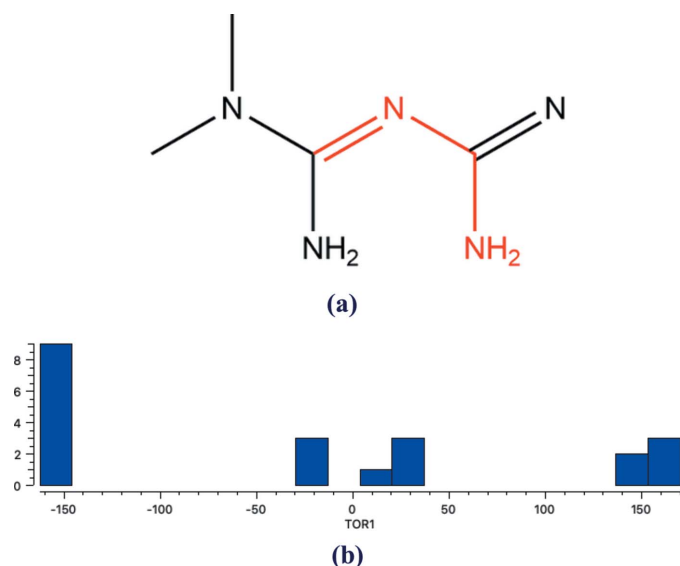


Figure 9
 (a) Fragment used for search in Cambridge Structural Database, (b) histogram of torsion angle TOR1 [shown in red in (a)].

for the N-containing part of the title compound, as shown in Fig. 9a resulted in 17 hits [DEXBUF and DEXBUF01 (Nanubolu *et al.*, 2013), DELKAK (Diniz *et al.*, 2022), EQUATIV (Olar *et al.*, 2010a), EWISAH (Polito-Lucas *et al.*, 2021), JUMXOH (Bian *et al.*, 2020), MAXJAA (Sun *et al.*, 2022), NAKWAB (Manjunatha *et al.*, 2020), NICCEJ (Satyanarayana Reddy *et al.*, 2013), NUPXED (Dong *et al.*, 2015), OJOSUC (Olar *et al.*, 2010b), OJOSUC01 (Wei *et al.*, 2014), QILBOF (Sánchez-Lara *et al.*, 2018), ROLFUV (Jia *et al.*, 2019), UKODUW01 (Feng *et al.*, 2021), WBSIJ (Lemoine *et al.*, 1994), YEJVOC (Jiang *et al.*, 2022); for more details, see the supporting information]. In contrast to the title compound, all 17 compounds bear a positive charge. The histogram of the torsion angle TOR1 illustrates that the majority of these fragments are non-planar (Fig. 9b). For the title compound, this torsion angle is $-177.5(4)$ and $-171.8(4)^\circ$ in A and B, respectively.

5. Synthesis and crystallization

The reaction scheme to synthesize the title compound is given in Fig. 10.

Metformin hydrochloride (662.5 mg, 4.0 mmol) was dissolved in 1M sodium hydroxide solution (320 ml, 8.0 mmol). The mixture was stirred for 30 min at room temperature. After the reaction was complete, water was removed under reduced pressure and the residue was dissolved in cold anhydrous methanol. The sodium chloride was filtered off and the filtrate was evaporated under reduced pressure to obtain basic metformin.

The basic metformin (258.2 mg, 2.0 mmol) and 3-bromobenzenesulfonyl chloride (144 μL , 1.0 mmol) were dissolved in 6 mL of anhydrous dichloromethane and stirred under a nitrogen atmosphere for 3 h at room temperature. The solvent was removed on a rotary evaporator and the residue was

purified by column chromatography (eluent: MeOH: $\text{CH}_2\text{Cl}_2 = 1:10$) to obtain the title compound as a colourless solid.

To obtain its hydrochloride salt, the title compound was dissolved in ethanol and stirred at room temperature. An ethanol solution of hydrochloric acid was added dropwise until $\text{pH} = 2$ and the reaction was followed by TLC. After completion of the reaction, the solvent was removed under reduced pressure to obtain the hydrochloride salt.

The hydrochloride salt (76.7 mg, 0.2 mmol) and sodium glioclazide (69.3 mg, 0.2 mmol) were dissolved in 5 mL of acetone and stirred overnight at room temperature. The solvent was removed under reduced pressure and a light-yellow solid was obtained, which was expected to be the sulfonylurea salt of the title compound.

Cuboid-shaped colourless crystals were grown in an NMR tube by slow evaporation over two weeks using deuterated chloroform as solvent. However, the grown crystals consist of the title compound and not of its sulfonylurea salt.

NMR spectra of the title compound were recorded on a 400 MHz NMR spectrometer: ^1H NMR (400 MHz, CDCl_3) δ 8.03 (*t*, $J = 1.7$ Hz, 1H, phenyl), 7.90–7.76 (*m*, 1H, phenyl), 7.64–7.57 (*m*, 1H, phenyl), 7.56–7.22 (*m*, 3H, phenyl and NH_2), 7.06 (*s*, 1H, NH_2), 5.19 (*s*, 1H, NH_2), 2.99 (*s*, 6H, CH_3). ^{13}C NMR (101 MHz, CDCl_3) δ 160.29 (*s*), 158.59 (*s*), 145.65 (*s*), 134.41 (*s*), 130.20 (*s*), 129.13 (*s*), 124.70 (*s*), 122.54 (*s*), 37.00 (*s*).

6. Refinement

Crystal data, data collection and structure refinement details are summarized in Table 3. All hydrogen atoms bound to carbon were placed at idealized positions and refined using a riding model, with $U_{\text{iso}}(\text{H})$ values assigned as $1.2U_{\text{eq}}$ or $1.5U_{\text{eq}}$ (methyl only) of the parent atoms, with C–H distances of 0.93 (aromatic) and 0.96 Å (methyl). The hydrogen atoms bound to nitrogen were located in a difference-Fourier map and

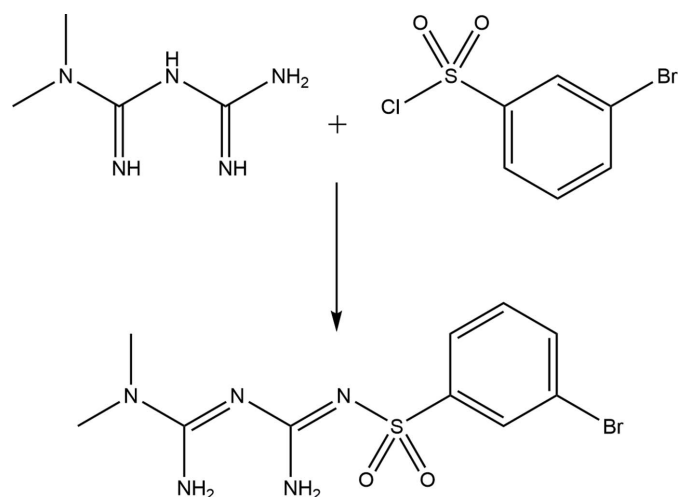


Figure 10
 Reaction scheme for the synthesis of the title compound.

Table 3
Experimental details.

Crystal data	
Chemical formula	C ₁₀ H ₁₄ BrN ₅ O ₂ S
<i>M_r</i>	348.23
Crystal system, space group	Triclinic, <i>P</i> $\bar{1}$
Temperature (K)	294
<i>a</i> , <i>b</i> , <i>c</i> (Å)	10.3839 (5), 11.3296 (6), 12.3477 (7)
α , β , γ (°)	103.393 (5), 96.380 (4), 97.934 (4)
<i>V</i> (Å ³)	1384.10 (13)
<i>Z</i>	4
Radiation type	Mo <i>K</i> α
μ (mm ⁻¹)	3.13
Crystal size (mm)	0.6 × 0.3 × 0.3
Data collection	
Diffraction	SuperNova, Single source at offset/ far, Eos
Absorption correction	Multi-scan (<i>CrysAlis PRO</i> ; Rigaku OD, 2022)
<i>T</i> _{min} , <i>T</i> _{max}	0.417, 1.000
No. of measured, independent and observed [<i>I</i> > 2σ(<i>I</i>)] reflections	16803, 5658, 3549
<i>R</i> _{int}	0.051
(sin θ/λ) _{max} (Å ⁻¹)	0.625
Refinement	
<i>R</i> [<i>F</i> ² > 2σ(<i>F</i> ²)], <i>wR</i> (<i>F</i> ²), <i>S</i>	0.053, 0.117, 1.02
No. of reflections	5658
No. of parameters	372
H-atom treatment	H atoms treated by a mixture of independent and constrained refinement
$\Delta\rho_{\max}$, $\Delta\rho_{\min}$ (e Å ⁻³)	1.05, -0.88

Computer programs: *CrysAlis PRO* (Rigaku OD, 2022), *SHELXT2014/5* (Sheldrick, 2015a), *SHELXL2016/4* (Sheldrick, 2015b) and *OLEX2* (Dolomanov et al., 2009).

refined freely with *U*_{iso}(H) values assigned as 1.2*U*_{eq} of the parent atoms. The occupancy factors of hydrogen atoms H11 and H15*B* (molecule *A*), and H30 and H34*B* (molecule *B*) involved in intramolecular hydrogen bonds converged during refinement to 0.85 (4) for H15*B* and H34*B*, and 0.15 (4) for H11 and H30.

Acknowledgements

The authors thank Bingyu Li and Professor Wim De Borggraeve for assistance with the synthesis.

Funding information

KS thanks the Chinese Scholarship Council for a CSC Fellowship and LVM the Hercules Foundation for supporting the purchase of the diffractometer through project AKUL/09/0035. JL acknowledges the Sichuan Science and Technology Program (project No. 2022ZYD0016 and 2023JDRC0013), and the National Natural Science Foundation of China (project No. 21776120).

References

Barzilai, N., Crandall, J., Kritchevsky, S. & Espeland, M. (2016). *Cell Metab.* **23**, 1060–1065.

Bian, X., Jiang, L., Zhou, J., Guan, X., Wang, J., Xiang, P., Pan, J. & Hu, X. (2020). *Molecules*, **25**, 1343.

Diniz, L. F., Carvalho, P. S., Gonçalves, J. E., Diniz, R. & Fernandes, C. (2022). *New J. Chem.* **46**, 13725–13737.

Dolomanov, O. V., Bourhis, L. J., Gildea, R. J., Howard, J. A. K. & Puschmann, H. (2009). *J. Appl. Cryst.* **42**, 339–341.

Dong, J., Liu, B. & Yang, B. (2015). *Acta Cryst.* **E71**, o747–o748.

Etter, M. C., MacDonald, J. C. & Bernstein, J. (1990). *Acta Cryst.* **B46**, 256–262.

Feng, W., Wang, L., Gao, J., Zhao, M., Li, Y., Wu, Z. & Yan, C. (2021). *J. Mol. Struct.* **1234**, 130166.

Giannarelli, R., Aragona, M., Coppelli, A. & Del Prato, S. (2003). *Diabetes Metab.* **29**, 6S2, 8–635.

Groom, C. R., Bruno, I. J., Lightfoot, M. P. & Ward, S. C. (2016). *Acta Cryst.* **B72**, 171–179.

Jia, L., Wu, S. & Gong, J. (2019). *Acta Cryst.* **C75**, 1250–1258.

Jiang, L., Hu, X. & Cai, L. (2022). *Molecules*, **27**, 3472.

Jing, Y., Wu, F., Li, D., Yang, L., Li, Q. & Li, R. (2018). *Mol. Cell Endocrinol.* **461**, 256–264.

Lemoine, P., Tomas, A., Viossat, B., Dung, N.-H. (1994). *Acta Cryst.* **C50**, 1437–1439.

Libby, G., Donnelly, L. A., Donnan, P. T., Alessi, D. R., Morris, A. D. & Evans, J. M. (2009). *Diabetes Care*, **32**, 1620–1625.

Lin, H. Z., Yang, S. Q., Chuckaree, C., Kuhajda, F., Ronnet, G. & Diehl, A. M. (2000). *Nat. Med.* **6**, 998–1003.

Lord, J., Flight, I. H. K. & Norman, R. J. (2003). *BMJ*, **327**, 951–955.

Manjunatha, N. K., Mahesha, Gayathri, B. H., Lokanath, N. K., Swamy, M. T., Chandra Nayaka, S., Siddaraju, B. P., Ragini, N., Al-Ghorbani, M., Kannika, B. R. & Madan Kumar, S. (2020). *Chem. Data Collect.* **30**, 100577.

Nanubolu, J. B., Sridhar, B., Ravikumar, K., Sawant, K. D., Naik, T. A., Patkar, L. N., Cherukuvada, S. & Sreedhar, B. (2013). *CrystEngComm*, **15**, 4448–4464.

Olar, R., Badea, M., Grecu, M. N., Balotescu, C.-M., Marinescu, D., Iorgulescu, E.-E., Lazar, V. & Bleotu, C. (2010a). *Anal. Univ. Bucuresti Chim.* **19**, 13.

Olar, R., Badea, M., Marinescu, D., Chifiriuc, C., Bleotu, C., Grecu, M. N., Iorgulescu, E. E., Bucur, M., Lazar, V. & Finaru, A. (2010b). *Eur. J. Med. Chem.* **45**, 2868–2875.

Polito-Lucas, J. A., Núñez-Ávila, J. A., Bernès, S. & Pérez-Benítez, A. (2021). *IUCrData*, **6**, x210634.

Rena, G. & Lang, C. C. (2018). *Circulation*, **137**, 422–424.

Rigaku OD (2022). *CrysAlis PRO*. Rigaku Oxford Diffraction, Yarnton, England.

Sánchez-Lara, E., Treviño, S., Sánchez-Gaytán, B. L., Sánchez-Mora, E., Eugenia Castro, M., Meléndez-Bustamante, F. J., Méndez-Rojas, M. A. & González-Vergara, E. (2018). *Front. Chem.* **6**, 402.

Sarkar, A., Tiwari, A., Bhasin, P. S. & Mitra, M. (2011). *J. Appl. Pharm. Sci.* **1**, 11–19.

Satyanarayana Reddy, J., Ravikumar, N., Gaddamanugu, G., Naresh, K. N., Rajan, S. S. & Anand Solomon, K. (2013). *J. Mol. Struct.* **1039**, 137–143.

Sheldrick, G. M. (2015a). *Acta Cryst.* **A71**, 3–8.

Sheldrick, G. M. (2015b). *Acta Cryst.* **C71**, 3–8.

Spackman, P. R., Turner, M. J., McKinnon, J. J., Wolff, S. K., Grimwood, D. J., Jayatilaka, D. & Spackman, M. A. (2021). *J. Appl. Cryst.* **54**, 1006–1011.

Sun, J., Jia, L., Wang, M., Liu, Y., Li, M., Han, D. & Gong, J. (2022). *Cryst. Growth Des.* **22**, 1005–1016.

Wei, X., Fan, Y., Bi, C., Yan, X., Zhang, X. & Li, X. (2014). *Bull. Korean Chem. Soc.* **35**, 3495–3501.

supporting information

Acta Cryst. (2023). E79, 367-372 [https://doi.org/10.1107/S2056989023002165]

Crystal structure and Hirshfeld surface analysis of *N*-{*N*-[amino(dimethylamino)methyl]carbamimidoyl}-3-bromobenzenesulfonamide

Kexin Su, Jiangshui Luo and Luc Van Meervelt

Computing details

Data collection: *CrysAlis PRO* 1.171.42.73a (Rigaku OD, 2022); cell refinement: *CrysAlis PRO* 1.171.42.73a (Rigaku OD, 2022); data reduction: *CrysAlis PRO* 1.171.42.73a (Rigaku OD, 2022); program(s) used to solve structure: *SHELXT2014/5* (Sheldrick, 2015a); program(s) used to refine structure: *SHELXL2016/4* (Sheldrick, 2015b); molecular graphics: Olex2 1.3 (Dolomanov *et al.*, 2009); software used to prepare material for publication: Olex2 1.3 (Dolomanov *et al.*, 2009).

N-{*N*-[Amino(dimethylamino)methyl]carbamimidoyl}-3-bromobenzenesulfonamide

Crystal data

$C_{10}H_{14}BrN_5O_2S$

$M_r = 348.23$

Triclinic, $P\bar{1}$

$a = 10.3839$ (5) Å

$b = 11.3296$ (6) Å

$c = 12.3477$ (7) Å

$\alpha = 103.393$ (5)°

$\beta = 96.380$ (4)°

$\gamma = 97.934$ (4)°

$V = 1384.10$ (13) Å³

$Z = 4$

$F(000) = 704$

$D_x = 1.671$ Mg m⁻³

Mo $K\alpha$ radiation, $\lambda = 0.71073$ Å

Cell parameters from 4121 reflections

$\theta = 2.8$ – 25.9 °

$\mu = 3.13$ mm⁻¹

$T = 294$ K

Block, colourless

$0.6 \times 0.3 \times 0.3$ mm

Data collection

SuperNova, Single source at offset/far, Eos diffractometer

Radiation source: micro-focus sealed X-ray tube, SuperNova (Mo) X-ray Source

Mirror monochromator

Detector resolution: 15.9631 pixels mm⁻¹

ω scans

Absorption correction: multi-scan (CrysAlisPro; Rigaku OD, 2022)

$T_{\min} = 0.417$, $T_{\max} = 1.000$

16803 measured reflections

5658 independent reflections

3549 reflections with $I > 2\sigma(I)$

$R_{\text{int}} = 0.051$

$\theta_{\max} = 26.4$ °, $\theta_{\min} = 2.5$ °

$h = -12 \rightarrow 12$

$k = -14 \rightarrow 14$

$l = -15 \rightarrow 15$

Refinement

Refinement on F^2

Least-squares matrix: full

$R[F^2 > 2\sigma(F^2)] = 0.053$

$wR(F^2) = 0.117$

$S = 1.02$

5658 reflections

372 parameters

0 restraints

Primary atom site location: dual

Hydrogen site location: mixed

H atoms treated by a mixture of independent and constrained refinement

$w = 1/[\sigma^2(F_o^2) + (0.035P)^2 + 1.4413P]$

where $P = (F_o^2 + 2F_c^2)/3$

$$(\Delta/\sigma)_{\max} < 0.001$$

$$\Delta\rho_{\max} = 1.05 \text{ e } \text{\AA}^{-3}$$

$$\Delta\rho_{\min} = -0.88 \text{ e } \text{\AA}^{-3}$$

Special details

Geometry. All esds (except the esd in the dihedral angle between two l.s. planes) are estimated using the full covariance matrix. The cell esds are taken into account individually in the estimation of esds in distances, angles and torsion angles; correlations between esds in cell parameters are only used when they are defined by crystal symmetry. An approximate (isotropic) treatment of cell esds is used for estimating esds involving l.s. planes.

Fractional atomic coordinates and isotropic or equivalent isotropic displacement parameters (\AA^2)

	<i>x</i>	<i>y</i>	<i>z</i>	$U_{\text{iso}}^*/U_{\text{eq}}$	Occ. (<1)
C1	−0.0600 (5)	0.7080 (4)	0.0460 (3)	0.0392 (11)	
C2	0.0355 (4)	0.6995 (4)	0.1296 (3)	0.0357 (11)	
H2	0.111511	0.758247	0.153617	0.043*	
C3	0.0135 (4)	0.5996 (4)	0.1764 (3)	0.0318 (10)	
C4	−0.0994 (5)	0.5123 (4)	0.1403 (4)	0.0442 (12)	
H4	−0.112981	0.445965	0.172576	0.053*	
C5	−0.1915 (5)	0.5246 (5)	0.0562 (4)	0.0530 (13)	
H5	−0.267409	0.465854	0.031437	0.064*	
C6	−0.1727 (5)	0.6219 (5)	0.0087 (4)	0.0469 (13)	
H6	−0.235200	0.629864	−0.048086	0.056*	
Br7	−0.03344 (6)	0.84386 (6)	−0.02036 (5)	0.0661 (2)	
S8	0.13699 (11)	0.58384 (11)	0.28223 (9)	0.0367 (3)	
O9	0.0932 (3)	0.4667 (3)	0.3068 (3)	0.0508 (9)	
O10	0.2597 (3)	0.5961 (3)	0.2382 (3)	0.0503 (9)	
N11	0.1473 (3)	0.6992 (3)	0.3852 (3)	0.0347 (9)	
H11	0.214239	0.756936	0.396878	0.042*	0.15 (4)
C12	0.0568 (4)	0.7124 (4)	0.4561 (3)	0.0337 (10)	
N13	0.0563 (3)	0.8161 (3)	0.5341 (3)	0.0324 (8)	
C14	0.1437 (4)	0.9194 (4)	0.5488 (3)	0.0308 (10)	
N15	0.2461 (4)	0.9308 (4)	0.4932 (4)	0.0435 (11)	
H15A	0.301 (5)	0.992 (5)	0.506 (4)	0.052*	
H15B	0.253 (5)	0.871 (5)	0.438 (5)	0.052*	0.85 (4)
N16	−0.0418 (5)	0.6209 (4)	0.4518 (4)	0.0513 (12)	
H16A	−0.088 (5)	0.634 (5)	0.500 (4)	0.062*	
H16B	−0.035 (5)	0.549 (5)	0.422 (4)	0.062*	
N17	0.1270 (3)	1.0179 (3)	0.6273 (3)	0.0364 (9)	
C18	0.0186 (5)	1.0110 (5)	0.6928 (4)	0.0543 (14)	
H18A	−0.035482	0.931202	0.666556	0.081*	
H18B	−0.033126	1.073065	0.684068	0.081*	
H18C	0.053284	1.024212	0.770841	0.081*	
C19	0.2135 (5)	1.1361 (4)	0.6488 (4)	0.0494 (13)	
H19A	0.303190	1.125183	0.663859	0.074*	
H19B	0.192002	1.192125	0.712777	0.074*	
H19C	0.202254	1.169086	0.584087	0.074*	
C20	0.5361 (5)	0.1808 (4)	0.0442 (4)	0.0398 (12)	
C21	0.4466 (4)	0.1344 (4)	0.1054 (3)	0.0359 (11)	
H21	0.356697	0.128306	0.084312	0.043*	

C22	0.4950 (4)	0.0973 (4)	0.1993 (3)	0.0311 (10)	
C23	0.6286 (5)	0.1067 (4)	0.2308 (4)	0.0484 (13)	
H23	0.660272	0.083478	0.294840	0.058*	
C24	0.7145 (5)	0.1507 (5)	0.1663 (5)	0.0645 (16)	
H24	0.804515	0.155822	0.186400	0.077*	
C25	0.6690 (5)	0.1871 (5)	0.0730 (5)	0.0527 (14)	
H25	0.727602	0.215887	0.029400	0.063*	
Br26	0.47490 (7)	0.23897 (6)	-0.08045 (5)	0.0725 (2)	
S27	0.38479 (12)	0.04014 (10)	0.28332 (9)	0.0356 (3)	
O28	0.4452 (3)	-0.0477 (3)	0.3299 (3)	0.0496 (9)	
O29	0.2591 (3)	-0.0032 (3)	0.2118 (3)	0.0467 (8)	
N30	0.3838 (3)	0.1539 (3)	0.3879 (3)	0.0343 (9)	
H30	0.428755	0.156416	0.451519	0.041*	0.15 (4)
C31	0.3160 (4)	0.2461 (4)	0.3813 (3)	0.0319 (10)	
N32	0.3220 (3)	0.3472 (3)	0.4660 (3)	0.0330 (8)	
C33	0.4065 (4)	0.3742 (4)	0.5619 (3)	0.0307 (10)	
N34	0.4890 (4)	0.3022 (4)	0.5916 (3)	0.0414 (10)	
H34A	0.550 (5)	0.327 (4)	0.648 (4)	0.050*	
H34B	0.486 (5)	0.234 (5)	0.543 (5)	0.050*	0.85 (4)
N35	0.2361 (4)	0.2468 (4)	0.2884 (3)	0.0434 (11)	
H35A	0.213 (5)	0.182 (4)	0.239 (4)	0.052*	
H35B	0.196 (5)	0.301 (4)	0.295 (4)	0.052*	
N36	0.4036 (4)	0.4825 (3)	0.6346 (3)	0.0418 (10)	
C37	0.3317 (5)	0.5744 (4)	0.6032 (4)	0.0510 (13)	
H37A	0.290176	0.544562	0.526308	0.076*	
H37B	0.391734	0.649473	0.611375	0.076*	
H37C	0.266048	0.589615	0.651189	0.076*	
C38	0.4763 (5)	0.5172 (5)	0.7476 (4)	0.0593 (15)	
H38A	0.473851	0.445938	0.777398	0.089*	
H38B	0.437222	0.578041	0.794622	0.089*	
H38C	0.565894	0.550465	0.745539	0.089*	

Atomic displacement parameters (Å²)

	U^{11}	U^{22}	U^{33}	U^{12}	U^{13}	U^{23}
C1	0.048 (3)	0.042 (3)	0.027 (2)	0.016 (3)	0.005 (2)	0.003 (2)
C2	0.035 (3)	0.036 (3)	0.033 (2)	0.005 (2)	0.002 (2)	0.002 (2)
C3	0.028 (3)	0.033 (3)	0.030 (2)	0.008 (2)	0.0028 (19)	-0.0012 (19)
C4	0.040 (3)	0.039 (3)	0.049 (3)	0.003 (2)	-0.001 (2)	0.009 (2)
C5	0.039 (3)	0.047 (3)	0.061 (3)	-0.003 (3)	-0.010 (3)	0.005 (3)
C6	0.037 (3)	0.057 (3)	0.040 (3)	0.014 (3)	-0.008 (2)	0.001 (3)
Br7	0.0806 (4)	0.0701 (4)	0.0497 (3)	0.0082 (3)	-0.0065 (3)	0.0297 (3)
S8	0.0382 (7)	0.0386 (7)	0.0329 (6)	0.0165 (6)	0.0017 (5)	0.0036 (5)
O9	0.070 (2)	0.0349 (19)	0.051 (2)	0.0233 (18)	0.0047 (18)	0.0108 (16)
O10	0.0370 (19)	0.070 (2)	0.0405 (18)	0.0223 (18)	0.0074 (15)	-0.0008 (17)
N11	0.033 (2)	0.038 (2)	0.0307 (19)	0.0037 (18)	0.0064 (17)	0.0028 (17)
C12	0.036 (3)	0.034 (3)	0.033 (2)	0.008 (2)	0.003 (2)	0.012 (2)
N13	0.035 (2)	0.030 (2)	0.0323 (19)	0.0048 (18)	0.0110 (17)	0.0060 (17)

C14	0.034 (3)	0.035 (3)	0.024 (2)	0.008 (2)	0.0017 (19)	0.0094 (19)
N15	0.040 (3)	0.041 (3)	0.042 (2)	-0.012 (2)	0.013 (2)	0.003 (2)
N16	0.060 (3)	0.031 (2)	0.061 (3)	-0.001 (2)	0.028 (2)	0.002 (2)
N17	0.036 (2)	0.035 (2)	0.035 (2)	0.0012 (19)	0.0055 (18)	0.0046 (17)
C18	0.057 (4)	0.048 (3)	0.058 (3)	0.012 (3)	0.028 (3)	0.003 (3)
C19	0.052 (3)	0.034 (3)	0.056 (3)	0.000 (3)	0.002 (3)	0.005 (2)
C20	0.058 (3)	0.030 (3)	0.033 (2)	0.011 (2)	0.013 (2)	0.006 (2)
C21	0.039 (3)	0.035 (3)	0.032 (2)	0.010 (2)	0.008 (2)	0.003 (2)
C22	0.034 (3)	0.027 (2)	0.029 (2)	0.005 (2)	0.007 (2)	0.0001 (18)
C23	0.043 (3)	0.054 (3)	0.054 (3)	0.010 (3)	0.007 (3)	0.025 (3)
C24	0.036 (3)	0.079 (4)	0.089 (4)	0.013 (3)	0.015 (3)	0.037 (4)
C25	0.051 (4)	0.047 (3)	0.068 (4)	0.009 (3)	0.026 (3)	0.021 (3)
Br26	0.1075 (5)	0.0769 (5)	0.0443 (3)	0.0238 (4)	0.0172 (3)	0.0299 (3)
S27	0.0461 (7)	0.0289 (6)	0.0326 (6)	0.0081 (6)	0.0128 (5)	0.0053 (5)
O28	0.075 (2)	0.0375 (19)	0.0488 (19)	0.0247 (18)	0.0270 (18)	0.0193 (16)
O29	0.043 (2)	0.045 (2)	0.0437 (19)	-0.0034 (16)	0.0109 (16)	-0.0031 (16)
N30	0.044 (2)	0.032 (2)	0.0283 (18)	0.0132 (18)	0.0067 (17)	0.0045 (16)
C31	0.032 (3)	0.033 (3)	0.031 (2)	0.005 (2)	0.010 (2)	0.008 (2)
N32	0.032 (2)	0.031 (2)	0.035 (2)	0.0084 (17)	0.0030 (17)	0.0033 (16)
C33	0.024 (2)	0.030 (2)	0.035 (2)	0.000 (2)	0.008 (2)	0.006 (2)
N34	0.039 (3)	0.040 (3)	0.037 (2)	0.008 (2)	-0.0092 (19)	0.001 (2)
N35	0.049 (3)	0.043 (3)	0.037 (2)	0.019 (2)	-0.002 (2)	0.0046 (19)
N36	0.049 (2)	0.034 (2)	0.036 (2)	0.007 (2)	0.0013 (19)	-0.0022 (18)
C37	0.056 (3)	0.032 (3)	0.060 (3)	0.006 (3)	0.008 (3)	0.002 (2)
C38	0.063 (4)	0.054 (3)	0.046 (3)	0.013 (3)	-0.005 (3)	-0.014 (3)

Geometric parameters (Å, °)

C1—C2	1.381 (6)	C20—C21	1.385 (6)
C1—C6	1.374 (6)	C20—C25	1.374 (7)
C1—Br7	1.906 (5)	C20—Br26	1.890 (4)
C2—H2	0.9300	C21—H21	0.9300
C2—C3	1.389 (6)	C21—C22	1.388 (6)
C3—C4	1.382 (6)	C22—C23	1.381 (6)
C3—S8	1.784 (4)	C22—S27	1.782 (4)
C4—H4	0.9300	C23—H23	0.9300
C4—C5	1.377 (6)	C23—C24	1.378 (7)
C5—H5	0.9300	C24—H24	0.9300
C5—C6	1.366 (7)	C24—C25	1.369 (7)
C6—H6	0.9300	C25—H25	0.9300
S8—O9	1.453 (3)	S27—O28	1.439 (3)
S8—O10	1.441 (3)	S27—O29	1.446 (3)
S8—N11	1.581 (4)	S27—N30	1.602 (3)
N11—H11	0.8600	N30—H30	0.8600
N11—C12	1.354 (5)	N30—C31	1.350 (5)
C12—N13	1.336 (5)	C31—N32	1.349 (5)
C12—N16	1.340 (6)	C31—N35	1.342 (6)
N13—C14	1.341 (5)	N32—C33	1.340 (5)

C14—N15	1.336 (5)	C33—N34	1.339 (5)
C14—N17	1.343 (5)	C33—N36	1.349 (5)
N15—H15A	0.80 (5)	N34—H34A	0.85 (5)
N15—H15B	0.86 (6)	N34—H34B	0.85 (6)
N16—H16A	0.80 (5)	N35—H35A	0.83 (5)
N16—H16B	0.83 (5)	N35—H35B	0.78 (5)
N17—C18	1.461 (5)	N36—C37	1.459 (6)
N17—C19	1.457 (6)	N36—C38	1.449 (6)
C18—H18A	0.9600	C37—H37A	0.9600
C18—H18B	0.9600	C37—H37B	0.9600
C18—H18C	0.9600	C37—H37C	0.9600
C19—H19A	0.9600	C38—H38A	0.9600
C19—H19B	0.9600	C38—H38B	0.9600
C19—H19C	0.9600	C38—H38C	0.9600
C2—C1—Br7	118.5 (4)	C21—C20—Br26	119.5 (4)
C6—C1—C2	122.4 (4)	C25—C20—C21	121.3 (4)
C6—C1—Br7	119.1 (3)	C25—C20—Br26	119.1 (4)
C1—C2—H2	121.4	C20—C21—H21	120.9
C1—C2—C3	117.2 (4)	C20—C21—C22	118.1 (4)
C3—C2—H2	121.4	C22—C21—H21	120.9
C2—C3—S8	118.3 (3)	C21—C22—S27	120.2 (3)
C4—C3—C2	121.2 (4)	C23—C22—C21	120.9 (4)
C4—C3—S8	120.4 (3)	C23—C22—S27	118.9 (3)
C3—C4—H4	120.3	C22—C23—H23	120.3
C5—C4—C3	119.3 (5)	C24—C23—C22	119.3 (5)
C5—C4—H4	120.3	C24—C23—H23	120.3
C4—C5—H5	119.6	C23—C24—H24	119.6
C6—C5—C4	120.8 (5)	C25—C24—C23	120.8 (5)
C6—C5—H5	119.6	C25—C24—H24	119.6
C1—C6—H6	120.5	C20—C25—H25	120.3
C5—C6—C1	119.0 (4)	C24—C25—C20	119.5 (5)
C5—C6—H6	120.5	C24—C25—H25	120.3
O9—S8—C3	105.9 (2)	O28—S27—C22	106.94 (19)
O9—S8—N11	114.05 (19)	O28—S27—O29	117.7 (2)
O10—S8—C3	106.56 (19)	O28—S27—N30	105.69 (19)
O10—S8—O9	116.50 (19)	O29—S27—C22	106.34 (19)
O10—S8—N11	106.7 (2)	O29—S27—N30	113.73 (18)
N11—S8—C3	106.42 (19)	N30—S27—C22	105.63 (19)
S8—N11—H11	118.1	S27—N30—H30	118.3
C12—N11—S8	123.7 (3)	C31—N30—S27	123.3 (3)
C12—N11—H11	118.1	C31—N30—H30	118.3
N13—C12—N11	123.7 (4)	N32—C31—N30	124.1 (4)
N13—C12—N16	114.6 (4)	N35—C31—N30	123.0 (4)
N16—C12—N11	121.7 (4)	N35—C31—N32	112.9 (4)
C12—N13—C14	123.6 (4)	C33—N32—C31	123.7 (4)
N13—C14—N17	116.7 (4)	N32—C33—N36	115.6 (4)
N15—C14—N13	125.2 (4)	N34—C33—N32	125.8 (4)

N15—C14—N17	118.1 (4)	N34—C33—N36	118.6 (4)
C14—N15—H15A	124 (4)	C33—N34—H34A	123 (3)
C14—N15—H15B	119 (4)	C33—N34—H34B	115 (4)
H15A—N15—H15B	117 (5)	H34A—N34—H34B	121 (5)
C12—N16—H16A	116 (4)	C31—N35—H35A	119 (3)
C12—N16—H16B	119 (4)	C31—N35—H35B	115 (4)
H16A—N16—H16B	120 (5)	H35A—N35—H35B	123 (5)
C14—N17—C18	120.9 (4)	C33—N36—C37	122.3 (4)
C14—N17—C19	121.8 (4)	C33—N36—C38	122.0 (4)
C19—N17—C18	117.3 (4)	C38—N36—C37	115.7 (4)
N17—C18—H18A	109.5	N36—C37—H37A	109.5
N17—C18—H18B	109.5	N36—C37—H37B	109.5
N17—C18—H18C	109.5	N36—C37—H37C	109.5
H18A—C18—H18B	109.5	H37A—C37—H37B	109.5
H18A—C18—H18C	109.5	H37A—C37—H37C	109.5
H18B—C18—H18C	109.5	H37B—C37—H37C	109.5
N17—C19—H19A	109.5	N36—C38—H38A	109.5
N17—C19—H19B	109.5	N36—C38—H38B	109.5
N17—C19—H19C	109.5	N36—C38—H38C	109.5
H19A—C19—H19B	109.5	H38A—C38—H38B	109.5
H19A—C19—H19C	109.5	H38A—C38—H38C	109.5
H19B—C19—H19C	109.5	H38B—C38—H38C	109.5
C1—C2—C3—C4	0.1 (6)	C20—C21—C22—C23	0.1 (6)
C1—C2—C3—S8	178.5 (3)	C20—C21—C22—S27	178.6 (3)
C2—C1—C6—C5	0.3 (7)	C21—C20—C25—C24	-2.2 (8)
C2—C3—C4—C5	0.2 (6)	C21—C22—C23—C24	-1.6 (7)
C2—C3—S8—O9	-174.6 (3)	C21—C22—S27—O28	149.4 (3)
C2—C3—S8—O10	-49.9 (4)	C21—C22—S27—O29	22.8 (4)
C2—C3—S8—N11	63.6 (4)	C21—C22—S27—N30	-98.3 (4)
C3—C4—C5—C6	-0.3 (7)	C22—C23—C24—C25	1.1 (8)
C3—S8—N11—C12	74.5 (4)	C22—S27—N30—C31	78.0 (4)
C4—C3—S8—O9	3.7 (4)	C23—C22—S27—O28	-32.1 (4)
C4—C3—S8—O10	128.4 (3)	C23—C22—S27—O29	-158.7 (4)
C4—C3—S8—N11	-118.0 (3)	C23—C22—S27—N30	80.1 (4)
C4—C5—C6—C1	0.0 (7)	C23—C24—C25—C20	0.7 (8)
C6—C1—C2—C3	-0.4 (6)	C25—C20—C21—C22	1.8 (7)
Br7—C1—C2—C3	180.0 (3)	Br26—C20—C21—C22	-177.3 (3)
Br7—C1—C6—C5	179.9 (4)	Br26—C20—C25—C24	176.9 (4)
S8—C3—C4—C5	-178.1 (4)	S27—C22—C23—C24	180.0 (4)
S8—N11—C12—N13	-171.1 (3)	S27—N30—C31—N32	-174.7 (3)
S8—N11—C12—N16	7.9 (6)	S27—N30—C31—N35	4.6 (6)
O9—S8—N11—C12	-41.9 (4)	O28—S27—N30—C31	-168.8 (3)
O10—S8—N11—C12	-172.0 (3)	O29—S27—N30—C31	-38.2 (4)
N11—C12—N13—C14	1.6 (6)	N30—C31—N32—C33	7.6 (7)
C12—N13—C14—N15	-4.1 (7)	C31—N32—C33—N34	-5.4 (7)
C12—N13—C14—N17	177.1 (4)	C31—N32—C33—N36	176.4 (4)
N13—C14—N17—C18	0.1 (6)	N32—C33—N36—C37	-10.9 (6)

N13—C14—N17—C19	-178.3 (4)	N32—C33—N36—C38	171.7 (4)
N15—C14—N17—C18	-178.7 (4)	N34—C33—N36—C37	170.8 (4)
N15—C14—N17—C19	2.8 (6)	N34—C33—N36—C38	-6.6 (6)
N16—C12—N13—C14	-177.5 (4)	N35—C31—N32—C33	-171.8 (4)

Hydrogen-bond geometry (Å, °)

<i>D</i> —H \cdots <i>A</i>	<i>D</i> —H	H \cdots <i>A</i>	<i>D</i> \cdots <i>A</i>	<i>D</i> —H \cdots <i>A</i>
N15—H15 <i>B</i> \cdots N11	0.86 (6)	2.02 (6)	2.655 (6)	130 (5)
N16—H16 <i>B</i> \cdots O9	0.83 (6)	2.19 (5)	2.830 (6)	134 (5)
N34—H34 <i>B</i> \cdots N30	0.86 (6)	2.02 (6)	2.696 (5)	135 (5)
N35—H35 <i>A</i> \cdots O29	0.83 (5)	2.18 (5)	2.823 (6)	136 (4)
N35—H35 <i>B</i> \cdots O9	0.78 (5)	2.27 (5)	3.049 (6)	175 (5)
N16—H16 <i>A</i> \cdots N32 ⁱ	0.81 (5)	2.54 (5)	3.225 (6)	144 (4)
N34—H34 <i>A</i> \cdots O10 ⁱⁱ	0.85 (5)	2.23 (5)	3.063 (5)	165 (4)

Symmetry codes: (i) $-x, -y+1, -z+1$; (ii) $-x+1, -y+1, -z+1$.